Method of measuring lateral deformation of hardening concrete specimen under monotonous and cyclic loading

P. Štemberk, A. Kohoutková

Czech Technical University in Prague, Faculty of Civil Engineering, Department of Concrete and Masonry Structures
Thákurova 7,166 29 Prague 6, Czech Republic, Phone: +420 224 354 364, E-mail: stemberk@fsv.cvut.cz.

Abstract

The measurement of lateral deformation of hardening concrete finds its application in many concrete technology fields, as it is used for direct derivation of the Poisson's ratio, which is necessary for multidimensional analyses. The soft consistency of hardening concrete prohibits any contact of a specimen with measuring equipment, therefore, a method using a CMOS camera to measure the lateral deformation of hardening concrete under uniaxial monotonous and cyclic loading is proposed. The presented method is based on processing of high-resolution images. The results obtained are in the form of a relation between the Poisson's ratio and the stress-strength ratio. Also, the issue related to the large amount of free water contained in the hardening concrete, which affects the measurement, is discussed and a corrective measure is suggested.

Keywords: hardening concrete, Poisson's ratio, stress-strength ratio, cyclic loading, monotonous loading, image processing.

Introduction

The measurement of lateral deformation of hardening concrete finds its application in many concrete technology fields. At present, however, there is no special testing method for measuring the lateral deformation of solidifying and further hardening concrete. Contact methods, which are used for already hardened concrete, are unsuitable for solidifying concrete due to either incapability of attaching measuring apparatus to the concrete surface or the lack of adhesion in the cases when embedded strain gauges are applied. The use of a laser sensor also is not easy to be applied since the longitudinal deformation of solidifying and further hardening concrete is rather large, which requires some mobile attachment of the laser sensor so that it can follow the targeted spot with progressing longitudinal deformation. Ultrasound measuring techniques represent a possible option for investigation of concrete characteristics at extremely early ages, such as evolution of the degree of hydration or the evolution of compressive strength, as evidenced in [1, 2]. However, they are not particularly suitable for measuring the lateral deformation of a concrete specimen as they do not solve the problems related to the pronounced longitudinal deformation. An optical method where the image is captured with a high resolution CMOS camera is relatively easy and nowadays also inexpensive. Capturing an image solves the part of acquiring test data on the lateral deformation, however, conversion of the image data to lateral deformation measurement requires some intention.

In this paper, we propose a method using a high-resolution CMOS camera to measure the lateral deformation of solidifying and hardening concrete under uniaxial monotonous and cyclic loading. The objective of the work is to measure the specimen's width under uniaxial monotonous and cyclic loading by a method which can be used at the ages just after the initial setting time when it is possible to demold a concrete specimen until the final setting time, when the standard measuring methods can be applied. The issues related to the large amount of water contained within solidifying concrete are also discussed.

Testing method

A CMOS camera (3456 x 2304 pixels) was used. In order to distinguish the edges of the specimen from the background, a dark curtain was installed behind the test set and the specimen was illuminated on both sides with two spotlights. The focus of the camera was set in advance and kept constant. The shutter of the camera was correlated in terms of time with a PC collecting data on longitudinal displacement (LVDT, stroke 200mm) and loading force (load cell). The loading force was imposed by an electric actuator. An example of a captured image is shown in Fig.1.

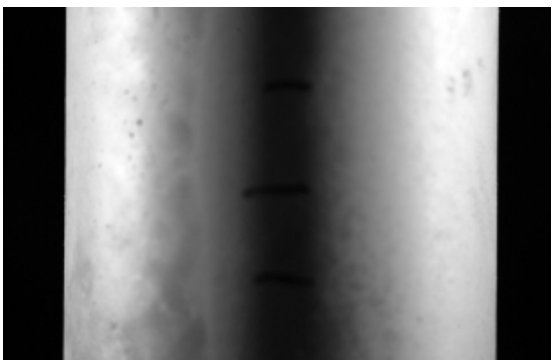

Fig.1 **Captured image of specimen**

Image processing

Three stripes were cut from a captured image. The monochromatic bitmap image comprising data in the form of 256 grades of gray scale was converted to an array of digits for each pixel. In order to detect the edges of the specimen, on the subpixel domain, the center of the gravity of the area under the curve defined by gray scale value differences of neighboring pixels was calculated. The distance between the centers of gravity on both sides of the specimen defined the width of a specimen. However, because the distance of the camera from a specimen was of about the same order as the width of the specimen, a

correction of the reading had to be introduced. More on the center of gravity method and the derivation of the correction of the reading can be found in [3]. The efficiency of the proposed method was verified by comparison with the approach proposed in [4], which was based on the polynomial fitting. The image processing can be summarized in the flowchart of the computer program:

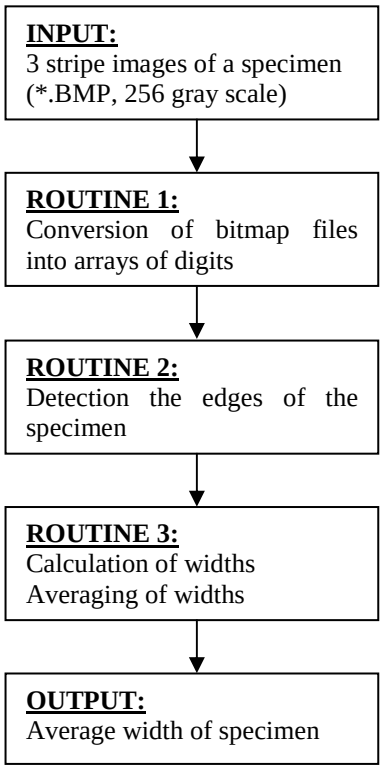

Input:

In order to minimize the effect of a local damage, the input batch consisted of three horizontal stripes cut out of the overall height of a specimen.

Routine 1:

The conversion of a bitmap into an array of digits can be achieved by selection of a proper function available in programming languages. The commonly used languages which are designed primarily for numerical calculations, such as the Fortran family, can import the graphics functions from other languages, such as C++. Matlab or Mathematica can be also used.

Routine 2:

The file obtained from the conversion of a rectangular image is usually in the format: the number of pixels in a row or a column, the values of pixels written row by row or column by column. For the edge detection it is necessary to exclude the effect of inhomogeneities caused, e.g. by voids in the surface of the specimen caused by air bubbles, which may delude the edge detecting routine. For this reason it is desirable to allow a height of a stripe of at least twice the size of the largest inhomogeneity near an edge. After averaging the pixel values in each column, a vector with the number of entries equal to the number of the column is obtained, in which 0 means black and 255 means white. Because the edge actually means the greatest difference between the gray shades of a specimen and the curtain, the vector is converted to a vector of the differences between neighboring pixels. The center of gravity should be calculated for an area which is limited by the length of 3-7 pixels near the initially localized edge on both sides of the pixel with the greatest value.

Routine 3:

The width of a specimen is calculated as the difference between the real number indicating the position of the entries in the vector of the differences which defines the edge on both sides of a specimen. The conversion into a real width is conducted with respect to the mm/pixel ratio. However, for the investigation of the Poisson's ratio, the conversion is not necessary since only the changes of the width corresponding with various load levels or various times are of interest.

Output:

The output of the program consists of three widths calculated for the three respective stripes, and the average width of the specimen.

More details about image processing techniques can be found in [3] or more generally in, e.g. [5].

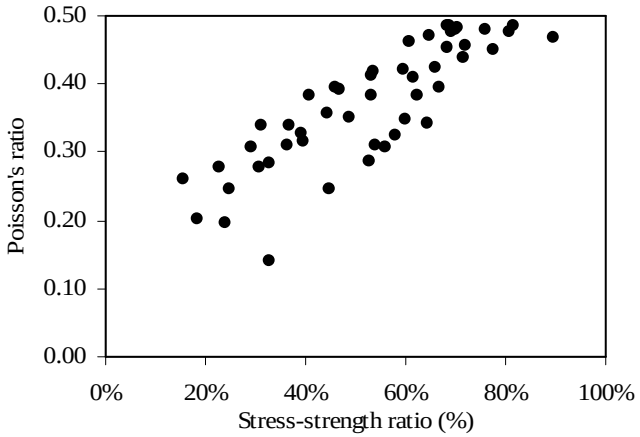

Fig.2. **Poisson's ratio under monotonous loading**

Experimental data

The experiment with monotonous loading was conducted with specimens (diameter = 100 mm and height = 200 mm) for two types of mixes using rapid hardening Portland cement (RHPC) of nominal 28-day compressive strengths of 30 MPa and 60 MPa. Those two mixes represent the minimum and maximum values of the compressive strength used in most civil engineering applications. The apparent Poisson's ratio, as a function of a load level for the two mixes is shown in Fig.2. Due to inconsistent reading of both the longitudinal and lateral deformations related to settling of the specimen at the beginning of loading, the reading of for stress-strength ratio less than about 20 % is omitted.

The experiment with cyclic loading was conducted with the same type of a specimen. The continuous longitudinal stress-strain curve is drawn in Fig.3. From this curve one can notice the pronounced irreversible deformation at higher load levels and partially reversible viscous behavior. The Poisson's ratio at cyclic loading is shown in Fig.4. The whole cycle is commonly perceived as the loop between zero-peak-zero loadings. The markers in Fig.4 correspond to the zero and peak loadings, therefore,

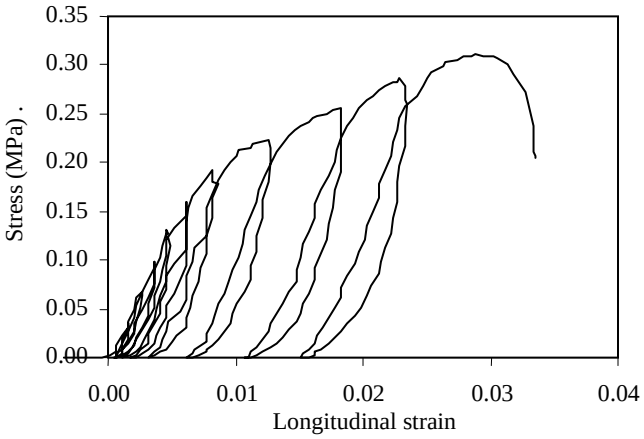

Fig.3 **Longitudinal stress-strain relation**

they are counted in half-cycles.

It can be observed in Figs.2 and 4 that the average Poisson's ratio of concrete of the age of 4 hours (counted from the instant when water touches cement) is higher than the usually considered values of 0.2. Also, it can be seen that at higher stress-strength ratios the Poisson's ratio exceeds the value 0.5 which corresponds with actual splitting of the specimen. Also, the Poisson's ratio is higher at peak loading than when unloaded for each load cycle, when at each cycle the peak load was increased by 50 kgf, which corresponds with the stress increase of 0.032 MPa. This is caused by the irreversible viscous behavior.

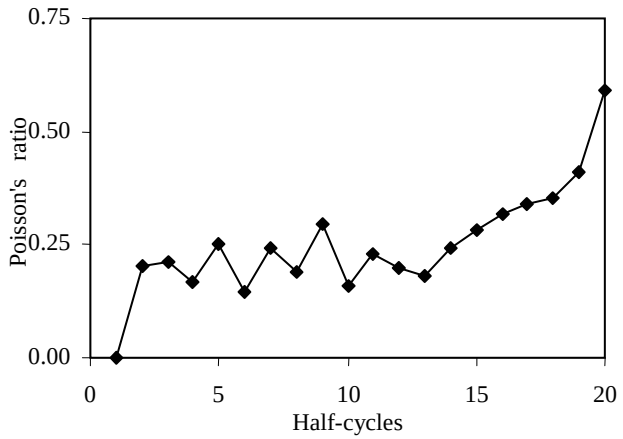

Fig.4 **Poisson's ratio under cyclic loading**

Discussion of accuracy

Because the result of this method was the relative difference between the original specimen's width and the width at a load step, it was not necessary to convert the calculated width in pixels to the width in, e.g. millimeters. The Poisson's ratio was then obtained as the ratio of the relative lateral deformation to the relative longitudinal deformation at each load step. Therefore, this method avoids errors stemming from conversion of pixels to millimeters.

It can be observed in Fig.2, which shows the Poisson's ratio as a function of stress-strength ratio, that for the stress-strength ratios below about 20 % the readings are missing. The data below 20 % were excluded as they showed inconsistent. The cause of the inconsistency was recognized as follows.

The hardening specimen (the age of concrete about 3 to 6 hours, counted from the instant when water touches cement) contains a large amount of free water (most of which later becomes chemically bound). Initially, before the loading starts, the free water is held inside the concrete specimen. When loading is applied, the free water is squeezed out of the specimen to its surface. Then, due to the heat emitted by spotlights the squeezed out water evaporates so that by the end of the experiment the surface of the specimen appears dry again. This sequence is shown in Fig.5. The squeezed out water reflects the light from the spotlights which changes the conditions in the edge detection, which eventually makes the specimen appear slimmer than it actually is.

Fig.2 shows that this problem affects only the region of stress-strength ratios below about 20 %. In the case of hardening concrete, it is imminent that some overloading, which means stress-strength ratios well above 50 %, will occur. Nevertheless, it is appropriate to explain the effect of wet and dry surface conditions on the results of measurements and assess its significance. To do so, a not loaded specimen was captured in a series of images before its surface was sprayed with water. Then, a series of images were taken while its surface was wet and eventually a series of images were taken in the course of time while the surface of the specimen was drying. This sequence is shown in Fig.5. The drying was rapid due to the heat from the spotlights and its actual duration is rather irrelevant, but it corresponded with reaching the stress-strength ratio of about 20 %.

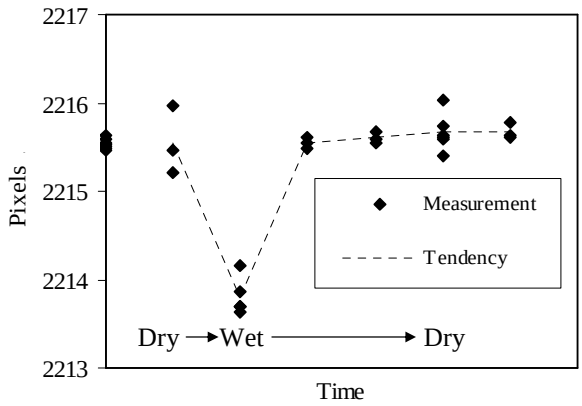

Fig.5. **Change in measured width of not loaded specimen**

In order to assess the error in measurement, the not loaded specimen was first captured in a series of images whose results are shown on the vertical axis in Fig.5. Here, it also can be seen that the method is fairly accurate as the scatter in the readings does not exceed a third of a pixel, while the width of the measured specimen was 2215.5 pixels, which means an error of 0.014 %. However, the measured differences in the width of the specimen under loading varied in the order of pixels, so the actual error in measurement can be estimated as up to 10 %. In this light, the error imposed by the change in the dry and wet surface

conditions is considerable as it results in unrealistic measurements shown as the dashed line in Fig.6. The specimen in Fig.6 was subjected to compression along its longitudinal axis, which in reality results in bulging of the specimen, i.e. the lateral strain increases positively. From this fact we derived the possible countermeasure.

Originally, it was tried to define some auto-correction function, but there seemed to be no way how to relate the differences in the images due to the wet and dry surfaces as the differences were measured from separate images. It was attempted to derive a function whose parameter was the sum of the gray-scale grades of pixels in the region near the edges, but there was no significant tendency recognized. Therefore, the results measured on the loaded specimens were rectified for the stress-strength ratios below 20 % by addition of the pixel difference recognized in Fig.5 for the wet surface with respect to an appropriate ratio of the width in pixels to the metric width, which took into account the effect of the distance of the camera from the specimen. In this way, it was possible to attain more realistic results which corresponded with the results obtained for the longitudinal deformation measurement.

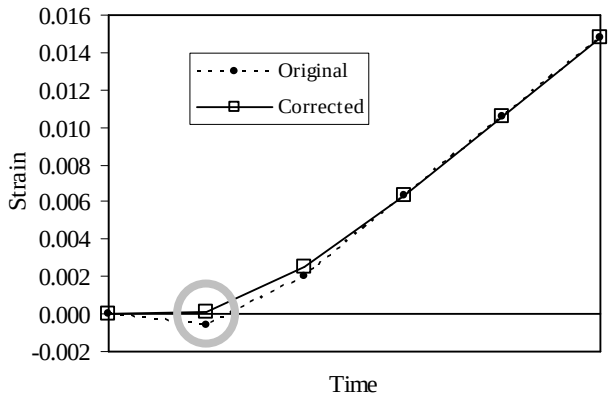

Fig.6. **Rectification of lateral strain**

As a result, the value of lateral strain, circled in Fig.6, became positive. The almost linear increase of strain over time in this case is correct since the loading was performed by constant increase of longitudinal deformation. The circled value in Fig.6 is not in the line with the subsequent readings which is due to the initial settlement of the specimen at the beginning of loading. The same situation was observed in the longitudinal strain.

This countermeasure is therefore effective as the realistic nature of the experimental data resumes.

Conclusions

A testing method was presented here which used a high-resolution CMOS camera for measuring lateral deformation of hardening concrete. The presented method proved effective and easy for use. The Poisson's ratio of hardening concrete subjected to uniaxial monotonous and cyclic loading for concrete at the ages between the initial and final setting time was investigated and the results were presented. The data were obtained for the ages between 3 and 6 hours. No significant tendency related to the progressing hydration was recognized.

The accuracy of the proposed method was also investigated and the method was found fairly accurate. It was recognized that the inconsistency in the readings for stress-strength ratios below 20 % was caused by the squeezed out water, which changed the surface conditions for the edge detection. An ad hoc solution was proposed which helped to restore the realistic look of the results. However, with respect to the test configuration and the loading procedure, the squeezed out water affected only the data for the stress-strength ratios below 20 %, while the range of application for hardening concrete begins at about the stress-strength ratio of 50 %. Therefore, it is assumed that the results obtained with the proposed method are valid for the ages ranging from the initial setting time (about 3 hours) to the final setting time (about 6 hours of age). In order to extend the range of application also for the stress-strength ratios below 20 %, the value of the Poisson's ratio can be estimated conservatively as constant 0.25.

Acknowledgement

This work was financially supported by the Ministry of Education, Youth and Sports of the Czech Republic, project number MSM6840770003, which is gratefully acknowledged.

References

1. **Öztürk T., Rapoport J., Popovics J. S. and Shah S. P.** Monitoring the setting and hardening of cement-based material with ultrasound. Concrete Science and Engineering. 1999. Vol.1(2). P. 83-91.
2. **Rapoport J., Popovics J. S., Subramaniam K. V. and Shah S. P.** The use of ultrasound to monitor the stiffening process of Portland cement concrete with admixtures. ACI Mat. J. 2000. Vol.97(6). P.675-683.
3. **Štemberk P. and Kohoutková A.** Image-analysis-based measuring of lateral deformation of hardening concrete. Materials Science (Medžiagotyra). 2005. Vol.11(3). P.292-296.
4. **Fu G. and Moosa A. G.** An optical approach to structure displacement measurement and its application. J. Eng. Mech., AMSE. 2002. Vol.128(5). P.511-520.
5. **Gonzalez R. and Woods R.** Digital Image Processing. Prentice-Hall, Inc. New Jersey. P.793. 2002.

Received 04 04 2006